Supporting Information

Interactions, properties and lipid digestibility of Attractive Pickering Emulgels formed by sequential addition of oppositely charged nanopolysaccharides

Shasha Guo,[a,b,c] Jun Li,[b] Xingxiang Ji,[a] Wenjuan Jiao,[d] Zhangmin Wan,[c] Luyao Huang,[b] Xun Niu,[c] Junhua Xu,[c] Ying Liu,[c] Jianan Zheng,[d] Bin Li,[e] Long Bai,[c,f] Yi Lu,[c,] Orlando J. Rojas [c,g,h,*]*

[a] State Key Laboratory of Biobased Material and Green Papermaking, Qilu University of Technology, Shandong Academy of Sciences, Jinan, 250353

[b] State Key Laboratory of Pulp and Paper Engineering, South China University of Technology, Guangzhou 510640, China

[c] Bioproducts Institute, Department of Chemical and Biological Engineering, University of British Columbia, 2360 East Mall, Vancouver BC V6T 1Z3, Canada

[d] Sericulture & Agri-food Research Institute Guangdong Academy of Agricultural Sciences, Key Laboratory of Functional Foods, Ministry of Agriculture and Rural Affairs, Guangdong Key Laboratory of Agricultural Products Processing, Guangzhou, 510610, China.

[e] CAS Key Laboratory of Biofuels, Qingdao Institute of Bioenergy and Bioprocess Technology, Chinese Academy of Sciences, Qingdao 266101, China

[f] Key Laboratory of Bio-based Material Science & Technology (Ministry of Education), Northeast Forestry University, Harbin 150040, P.R. China

[g] Department of Chemistry, 2036 Main Mall, The University of British Columbia, Vancouver BC V6T 1Z1, Canada

[h] Department of Wood Science, The University of British Columbia, 2900-2424 Main Mall Vancouver BC V6T 1Z4, Canada

[*] **Corresponding Authors:** Orlando J. Rojas, orlando.roja@ubc.ca; Yi Lu, yi.lu@ubc.ca

1. Experimental

1.1 Preparation and characterization of chitin nanofibrils (ChNF)

The process involved successive immersion of crab shells in 1 M HCl and 1 M NaOH for 24 h to remove minerals and proteins through at least three cycles. Subsequently, the obtained solids were decolorized by soaking in 0.5 wt% $NaClO_2$ solution (pH 5.0, acetic acid) for 2 h at 70°C. Purified chitin was obtained after thoroughly washing with distilled water. The chitin flakes were crushed into smaller pieces using a household blender and stored at 4°C for future use.

The purified chitin was then deacetylated with 33 wt% NaOH at 90°C for 3.5 h based on our previous report with minor modifications.[1] After that, partially deacetylated chitin was washed with Milli-Q water until the pH was constant, following an overnight dialysis to further remove impurities. The deacetylation degree of chitin was about 26%, similar to our early report.[2] The partially deacetylated chitin was re-dispersed in water (0.3 wt%), following pH adjustment using acetic acid to 3 under continuous stirring using a homogenizer (T-25, Digital Homogenizer, IKA, Germany). The dispersion of chitin nanofibrils was completed by a further 50 min ultrasonic treatment with a tip sonicator (Sonifier 450, Branson Ultrasonics Co., USA) for every 200-mL aliquot and following alternating on-off cycles (5 s - 2 s, respectively).

The morphology of CNC and ChNF was examined using transmission electron microscopy (TEM, FEI Tecnai G2S-Twin, USA) operating at an acceleration voltage of 80 kV. A colloidal suspension (0.01 wt%, 5 μL) was deposited on the Cu200 formvar/carbon grid for 30 s, excess water was removed using filter paper. Subsequently, the sample was stained with 2% uranyl acetate solution (5 μL), excess liquid was blotted with filter paper, and the sample was air-dried at room temperature.

1.2 QCM-D experiments

The QCM mass (Δm) of the adsorbed CNC was calculated from the change in frequency (Δf_n) and the energy dissipation (ΔD_n) at its 3rd overtone. CNC adsorption can be reflected by the mass variation calculated from frequency change (Δf_n) by using the Sauerbrey equation: [3]

$$\Delta m = -C\frac{\Delta f_n}{n} \quad \text{(S1)}$$

where C is the Sauerbrey constant for the mass sensitivity of quartz crystal (0.177 $mg \cdot Hz^{-1} \cdot cm^{-2}$ for a 5 MHz crystal) and n is the resonance overtone number (n = 3, 5, 7, 9, 11). Representative mass curves used for kinetics modeling are provided from the curves from the third overtone (n = 3) in this work.

1.3 Impact of CNC and ChNF adding sequence on the properties of Pickering emulsions

A two-step approach was applied to prepare the oil-in-water Pickering emulsions with 10 wt% oil, which includes the first nanoparticle emulsification, followed by continuous feeding of the secondary nanoparticle. In this section, CNC:ChNF = 5:1 (the net neutral system of CNC/ChNF suspension) was used to prepare Pickering emulsions. The concentrations of CNC and ChNF were 3.73 wt% and 0.75 wt% in final emulsions. Taking the Pickering stabilizer of CNC as an example, 8.4 g CNC suspension was mixed with 1 g oil, and then the mixture was ultrasonicated for 60 s. Additional experiments consisted of emulsions prepared via sequential ChNF addition by ultrasonicating for 30 s and stirring for 30 s. As a comparison, the mixture of CNC and oil was ultrasonicated for 90 s, following ChNF loading and stirring for 30 s. The lower oil fraction of 10 wt% was used in order to observe the creaming stability. The results provided a reference for the sequence and methods of adding two types of nanoparticles in subsequent experiments.

1.4 Classical molecular dynamics simulation (CMDS)

The α-chitin crystal was constructed based on the crystallographic vector investigated in earlier literature,[4] adopting the alpha-chitin-A configuration.[5] The α-chitin crystal has dimensions of 2.8494 nm, 3.778 nm, and 8.264 nm in the a, b, and c crystallographic parameter directions, respectively. To replicate our experimental procedure, the acetamidos on the (010) planes were altered to protonated aminos (-NH+ 3). The 18-chain cellulose I_β crystallite was constructed using crystallographic vectors derived from high-resolution X-ray data.[6] The crystallographic parameters for a, b, and c were determined to be 7.784, 8.201, and 10.38 nm, respectively. The γ angle was measured to be 96.5°. To mimic the nanocellulose employed in our research, we specifically select to modify the hydroxymethyl groups to sulfonates (-SO- 3) in both (110) and (010) crystallographic planes. The α-chitin crystal with A configuration and cellulose I_β crystallite were built by authors' awk script. Furthermore, the cyclohexane molecule was employed to represent the oil utilized in this investigation.

The CMD simulations described in this study were performed using Gromacs package,[7] version 2021.6, using the CHARMM36 Force Field for chitin and cellulose,[8] the TIP3P water model,[9] and the CHARMM General Force Field (CGenFF) for cyclohexane molecules.[10] The topology files were generated using CHARMM-GUI.[11] Initially, the complex system was neutralized with 0.15 M NaCl. Subsequently, energy minimization was performed using both steep descent and conjugate gradient approaches, with the maximal force converging to 100 kJ/mol/nm. An initial equilibrium simulation was conducted in the N.P.T. ensemble at a temperature of 303.[15] K and an ambient pressure of 1 bar. The simulation lasted for 1 ns in order to allow the water and oil molecules to reach equilibrium and eliminate any unrealistic overlaps between surrounding molecules. Next, the production simulation trajectories were propagated in the N.P.T. ensemble

for a duration of 100 ns. The particle mesh Ewald (PME) was consistently employed across all simulations to calculate long-range electrostatic interactions. The interactions that occur at small distances, such as Van der Waals interaction and short-range Coulombic interactions, were limited to a maximum distance of 1.2 nm.[12] The visualization in this study was conducted using the VMD package,[13] version 1.9.3. The investigation of non-covalent interaction energy was performed using the gmx energy utility.

1.5 Simulated gastrointestinal tract (GIT) model design

A fully designed single-stage *in vitro* digestion model, comprising the mouth, stomach, and small intestinal phases, was developed based on previous studies with certain modifications.[14] Prior to digestion, the enzyme activity and bile extract concentration were measured. The digestion process was conducted at a controlled temperature of 37°C with a rotational speed of 100 rpm (SHA-B, Lichen Technology, China). To avoid temperature variations, all solutions were preheated to 37°C. A test sample with a lower oil concentration (1 wt%) was prepared by dilution.

In the oral phase, 5 mL of the diluted emulsion was mixed with SSF, which contained 0.01875 g of mucin and 7.5 μmol of $CaCl_2 \cdot 2H_2O$ at a 1:1 (v/v) ratio. After pH adjustment to 7.0 using 5 M NaOH, the mixture was incubated for 6 min.

For the stomach stage, 10 mL of SGF, containing pepsin (2000 U mL^{-1} in the final mixture) and 0.15 mM $CaCl_2 \cdot 2H2O$, was added to the "bolus" from the oral phase. The pH was adjusted to 3.0 using 6 M HCl. Subsequently, the system was incubated for 2 h at 37°C.

In the small intestinal phase, the "chyme" from the gastric phase was diluted at a 1:1 (v/v) ratio with SIF. The SIF contained enzymes (pancreatin and pancreatic lipase) to achieve a trypsin activity of 100 U mL^{-1} and a lipase activity of 2000 U mL^{-1} in the final mixture. Additionally, it

contained 10 mM bile salts and 0.6 mM $CaCl_2 \cdot 2H_2O$. The pH was adjusted to approximately 7.0 using 5 M NaOH. The digestion process was performed with continuous shaking for 2 h.

2. Supporting Results

We first examine the influence of the stabilizer addition sequence and the mixing power on the stability of corresponding emulsions (1:9 oil-to-water ratio). **Figure S1** shows the properties of CNC-first Pickering emulsions by ultrasonication and stirring (i.e., adding CNC in Step 1, emulsifying the system, then adding ChNF in Step 2). The average droplet sizes (D_{32}) were 41.9 μm and 64.8 μm via ultrasonication and stirring, respectively. The Pickering emulsion with a strong mixing way of ChNF showed bimodal size distribution and clear serum after 7 days. The results indicated the second strong ultrasonication inputting could destroy CNC-stabilized Pickering emulsions following restructuring CNC, ChNF, or CNC/ChNF-stabilized Pickering emulsions. Cationic ChNF promoted some additional aggregation of the anionic CNC due to the heteroaggregation mechanism, which would result in the coalescence of the droplets under ultrasonication; on the other hand, neat ChNF-stabilized Pickering emulsion with a smaller size was generated, simultaneously.

In contrast, **Figure S2** shows the stability of ChNF-first Pickering emulsions (i.e., adding ChNF in Step 1, emulsifying the system, then adding CNC in Step 2). Changing the loading sequence had a significant impact on the emulsion morphology, as well as the mixing strategy. Stirring. Adding ChNF to CNC-stabilized Pickering emulsions using stirring, ChNF would rapidly absorb and bridge to the oil droplets (already covered by CNC) through electrostatic attraction, resulting in a droplet network. However, both protocols would cause the droplets to become significantly larger compared with ChNF-stabilized droplets (**Figure S2a**), which is not conducive to the stability of the subsequent emulsion.

Nevertheless, it must be denoted that we used only 10 wt.% oil content in these preliminary tests, merely for the purpose of indicating the impact of sequential addition and mixing power. The

low oil content facilitates the phase separation process, such that it is more obvious to identify the differences in emulsion stabilities. However, these emulsions here were not attractive Pickering emulsion gel (APEG) systems, since the oil content is too low to support a robust interdroplet bridging effect.

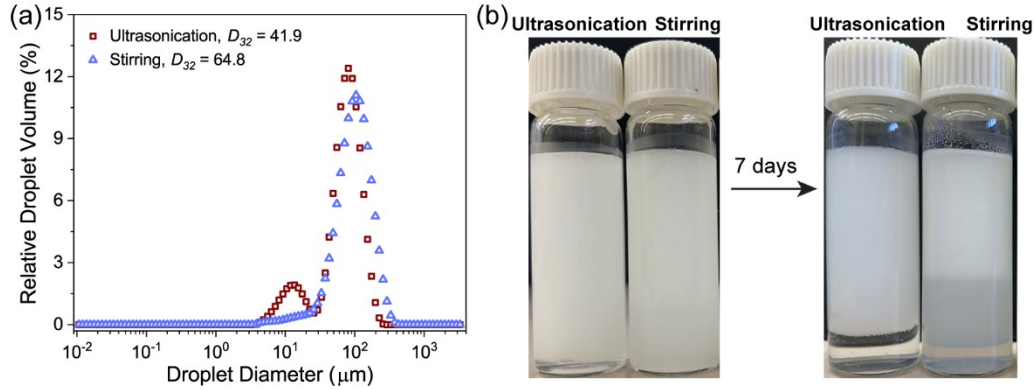

Fig. S1 CNC-stabilized Pickering emulsions with sequential ChNF addition by ultrasonication and stirring. (a) Size distribution of fresh Pickering emulsions and (b) Visual appearance at 0 day and 7 days.

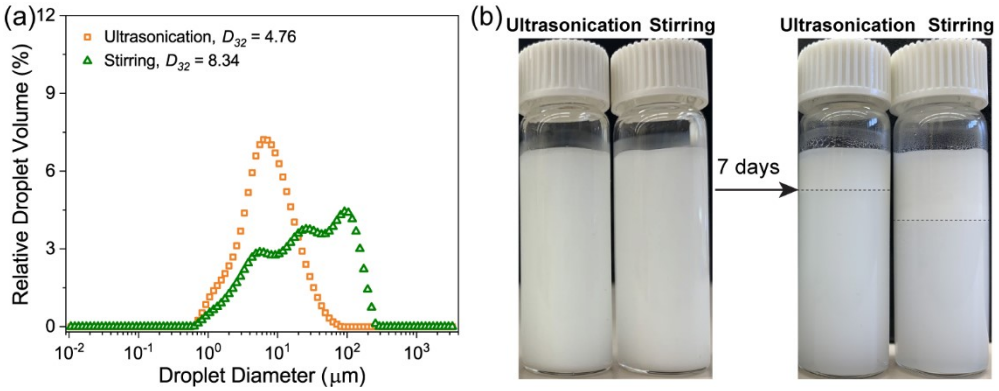

Fig. S2 ChNF-stabilized Pickering emulsions with sequential CNC addition by ultrasonication and stirring. (a) size distribution of fresh Pickering emulsions and (b) visual appearance at 0 day and 7 days.

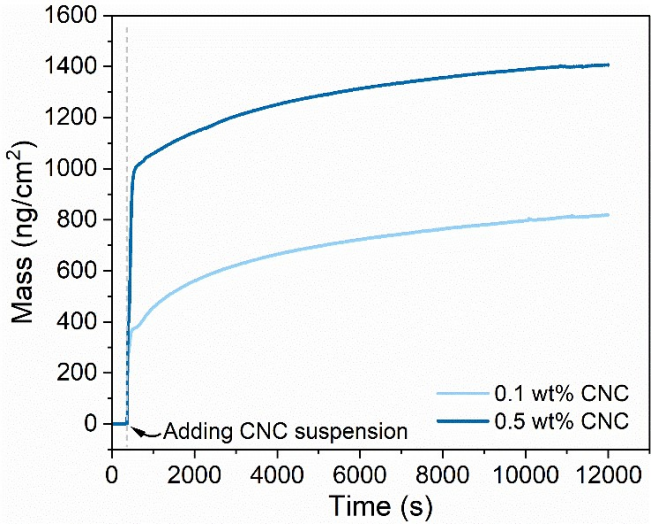

Fig. S3 ChNF-CNC sensogram obtained by a quartz-crystal microbalance with dissipation monitoring (QCM-D).

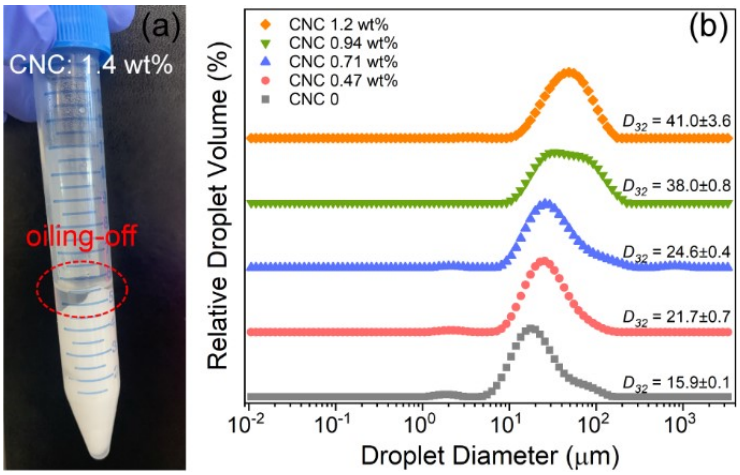

Fig. S4 (a) Photograph of ChNF-stabilized oil-in-water APEG with 1.4 wt% CNC. (b) Size distribution of ChNF-stabilized oil-in-water Pickering emulsion with given CNC loading of 0, 0.47, 0.71, 0.94, and 1.2 wt%.

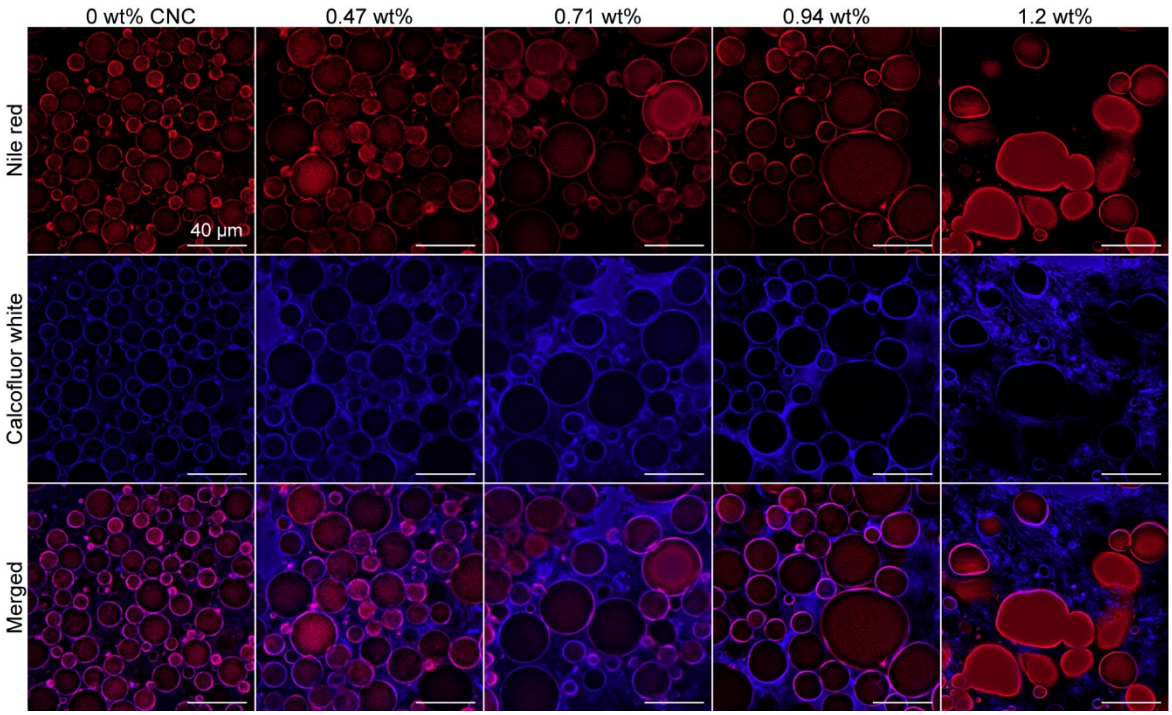

Fig. S5 Fluorescence microscopy images of ChNF-stabilized oil-in-water APEGs at CNC addition of 0, 0.47, 0.71, 0.94, and 1.2 wt%. When the oil phase (red) is emulsified in the water phase (blue), positively-charged ChNFs adsorbs at the oil-water interface, and then binds electrostatically with negatively-charged CNC.

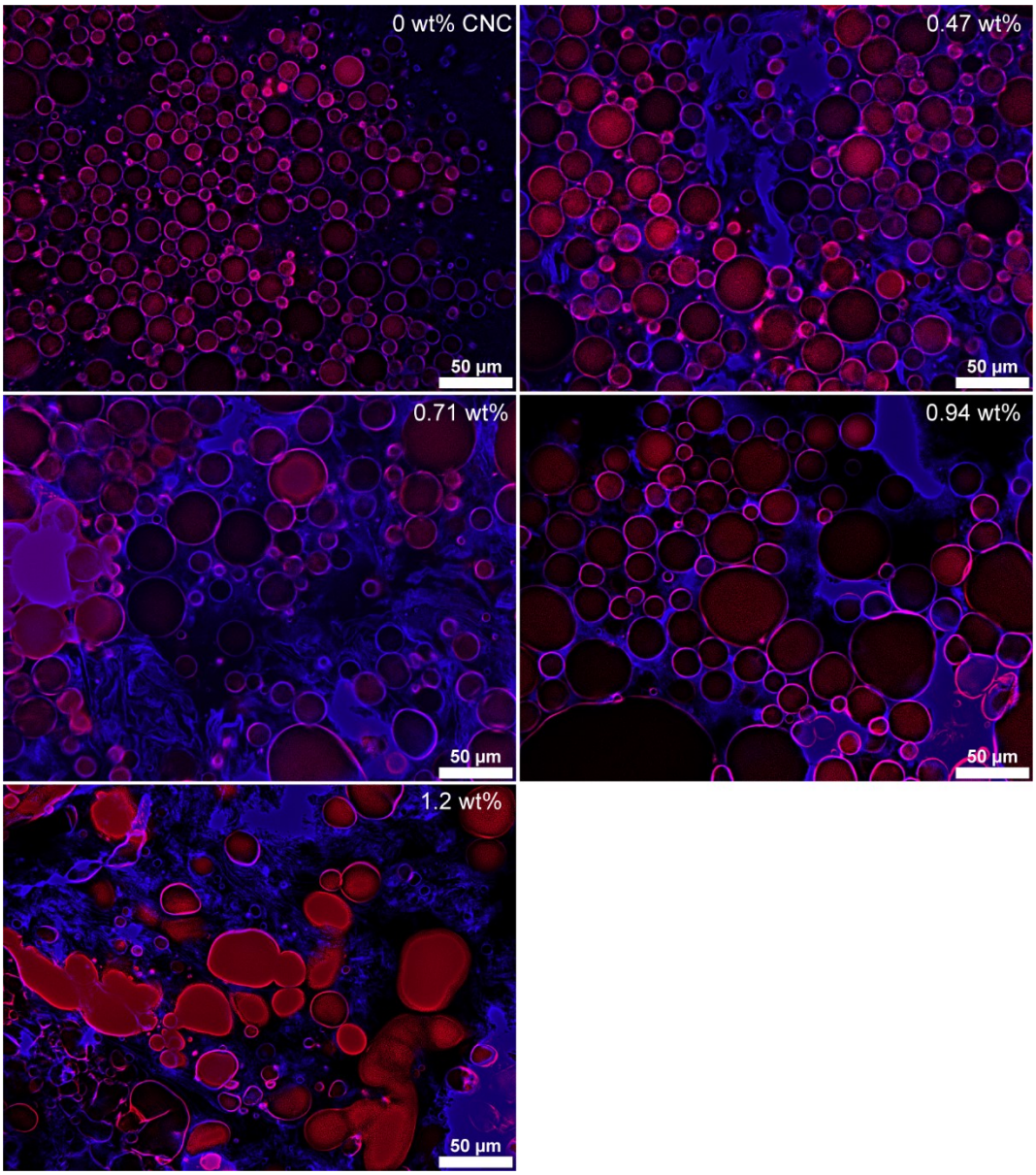

Fig. S6 Low magnified fluorescence images of ChNF-stabilized oil-in-water APEGs at CNC addition of 0, 0.47, 0.71, 0.94, and 1.2 wt%.

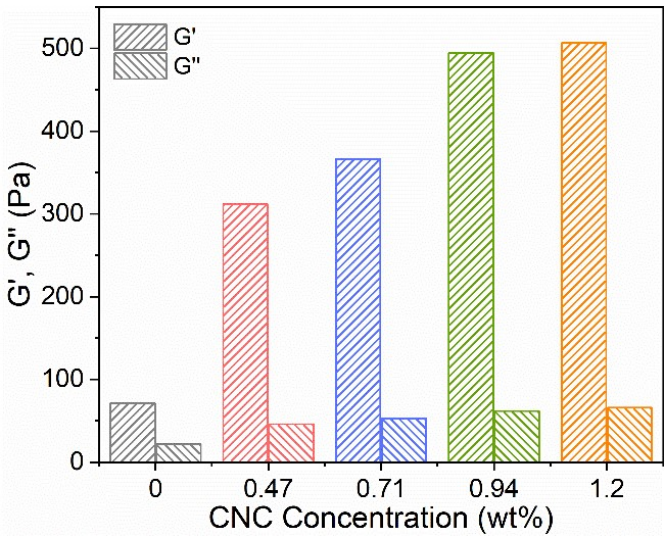

Fig. S7 Comparison of elastic (G') and viscous (G") moduli of APEGs formed with given CNC concentrations measured at a strain amplitude = 1.28% within the linear viscoelastic region.

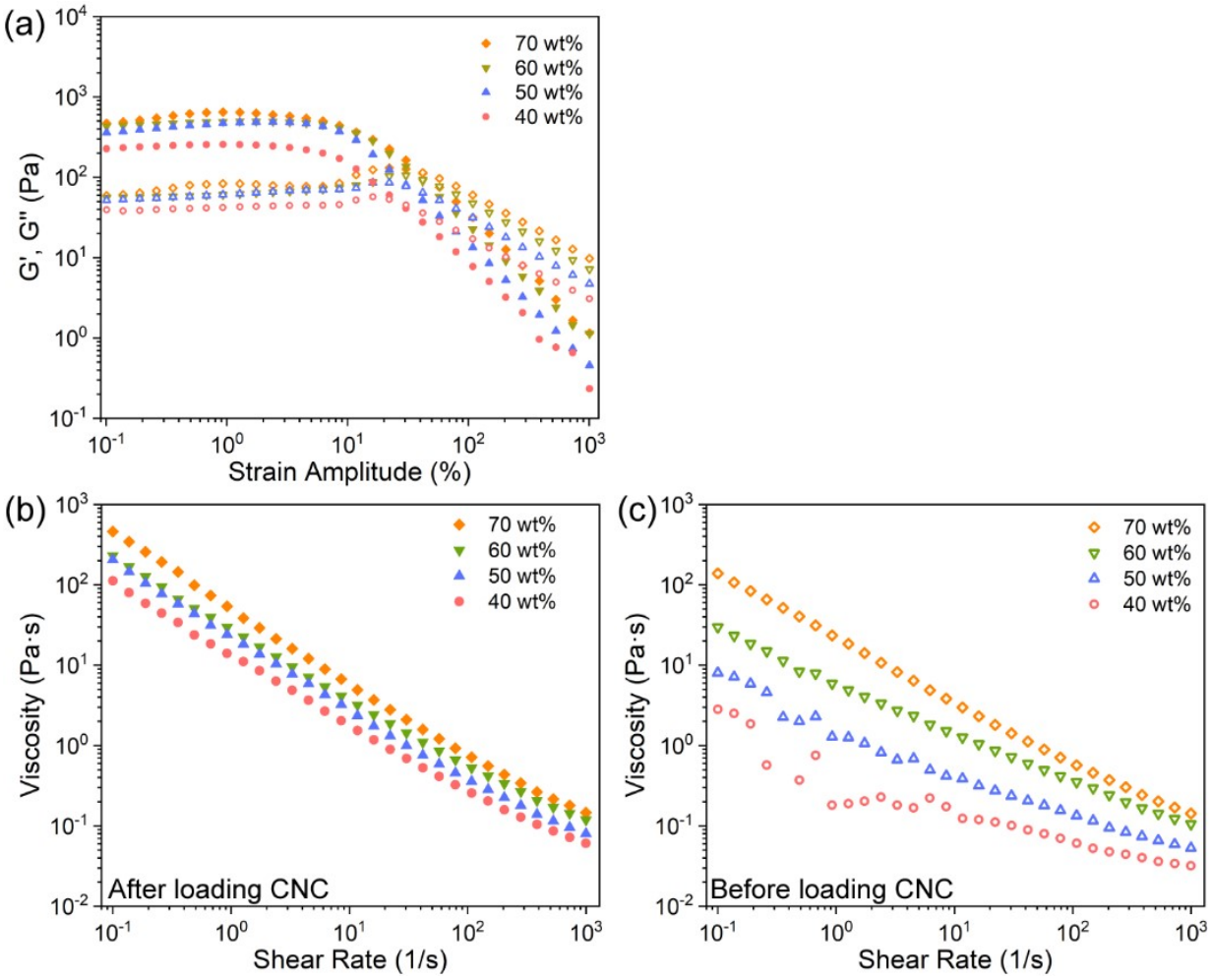

Fig. S8 (a) Strain amplitude sweep and (b) steady-state flow curves of APEGs with different oil fractions (40, 50, 60, and 70 wt%). (c) Steady-state flow curves of ChNF-stabilized Pickering emulsions without loading CNC. G' and G'' represent the elastic (storage) and viscous (loss) moduli, respectively.

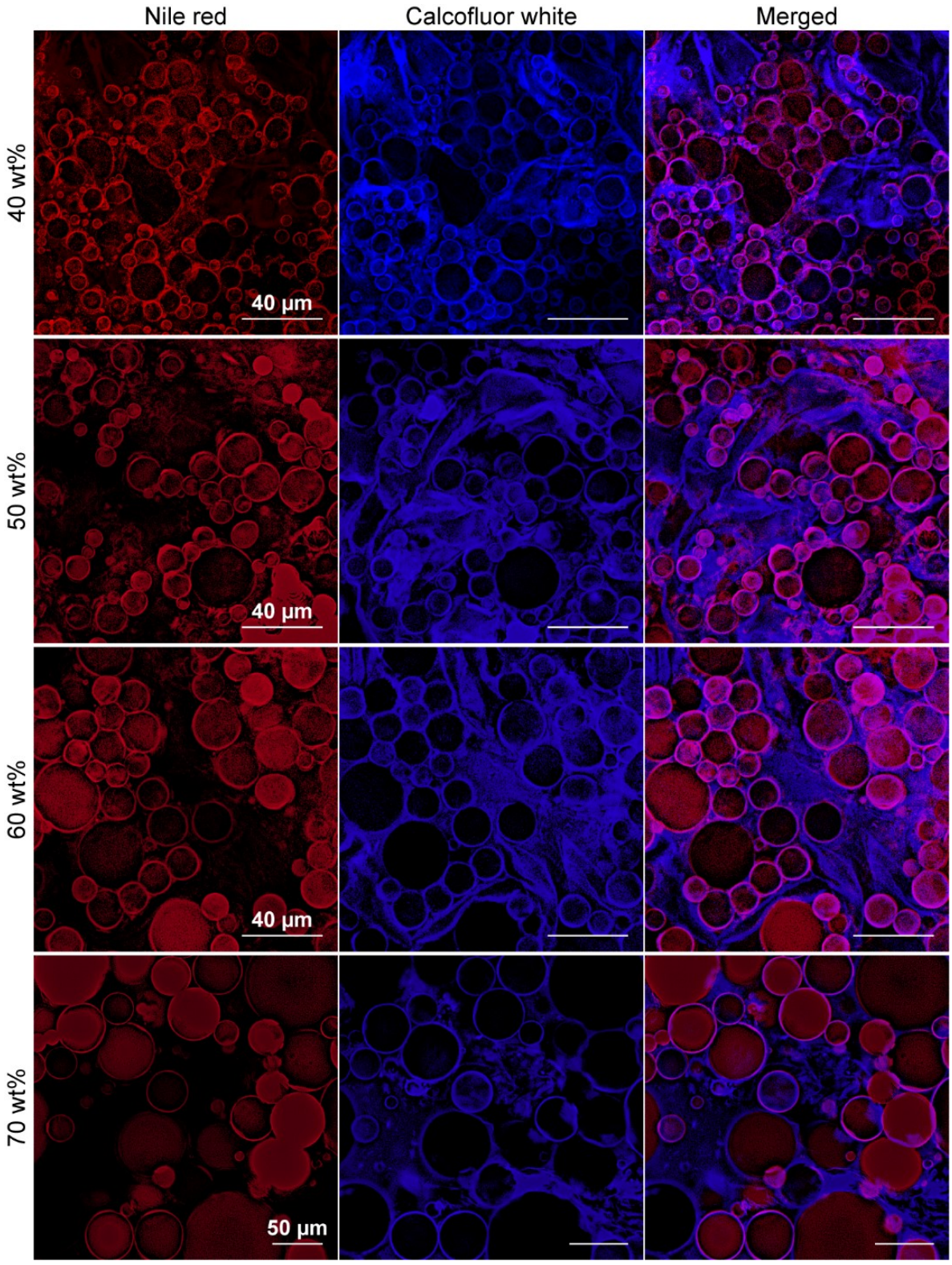

Fig. S9 Fluorescence microscopy images of ChNF-stabilized oil-in-water APEGs at different oil fractions (40, 50, 60, and 70 wt%).

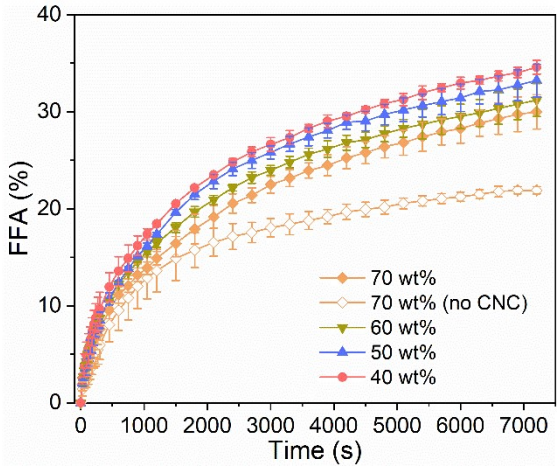

Fig. S10 Comparsion of FFA release between ChNF-CNC co-stabilized APEGs of different oil fraction (40, 50, 60, and 70 wt%, as noted) and the ChNF-stabilized Pickering emulsions of 70 wt% oil fraction without CNC.

Based on the literature available to us, this study represents the first digestion experiment of attractive Pickering emulsion gels constructed with ChNF and CNC. There were differences between the FFAs depending on the stabilizer type and level. Unlike conventional food-grade emulsifiers (gum arabic), APEGs showed better performance at inhibiting lipid digestion. The oil fractions of most chitin or cellulose based Pickering were around 5-15 wt%, and they have low viscosity and good fluidity. For comparison, APEGs showed a robust viscoelastic response and effectively conducted 3D printing.

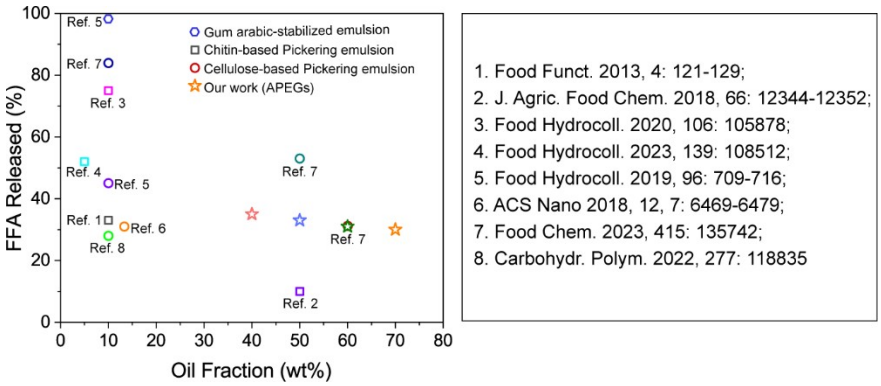

Fig. S11 Comparing the FFAs of APEGs and other published studies.

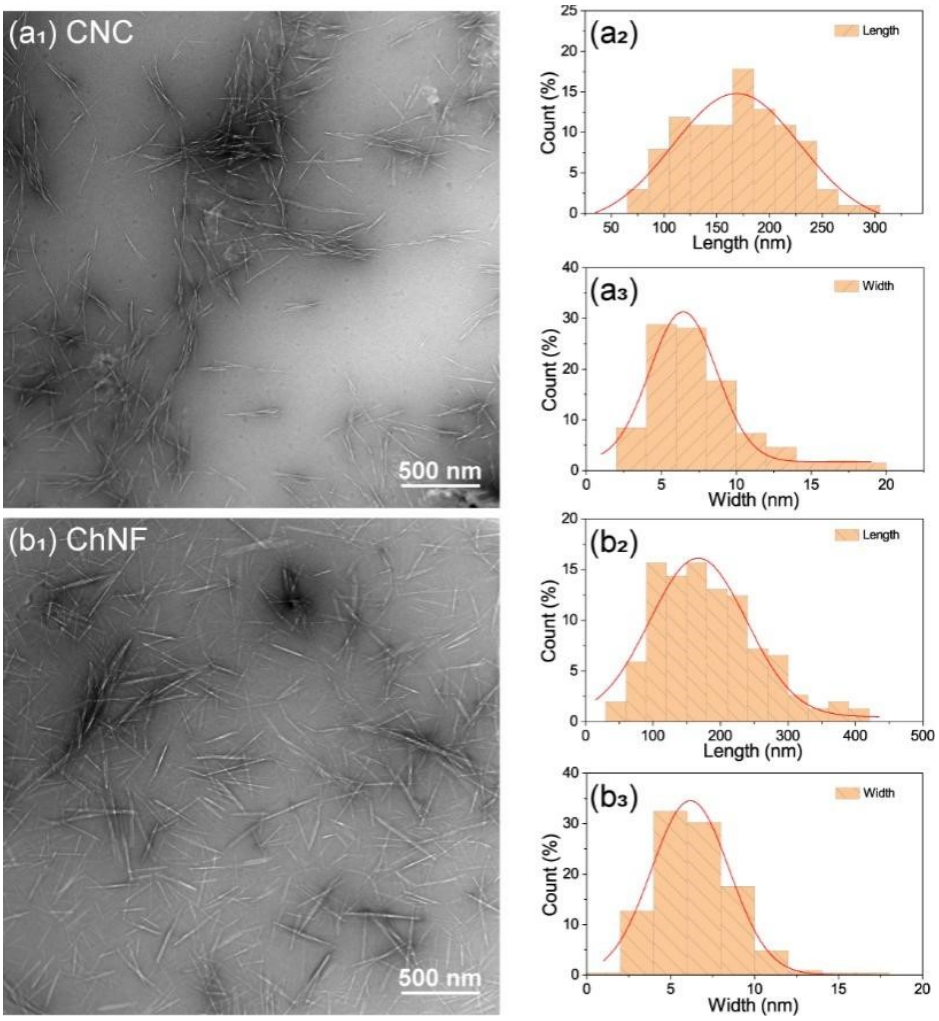

Fig. 12 TEM micrograph and size distribution of the CNC (a) and ChNF (b) used in this study. Red lines are the curves fitting the size distribution histogram.

References

1. S. Guo, Y. Zhu, W. Xu, S. Huan, J. Li, T. Song, L. Bai and O. J. Rojas, *Carbohydrate Polymers*, 2023, **299**, 120154.
2. S. Huan, Y. Zhu, W. Xu, D. J. McClements, L. Bai and O. J. Rojas, *ACS Applied Materials & Interfaces*, 2021, **13**, 12581-12593.
3. G. Sauerbrey, *Zeitschrift für Physik*, 1959, **155**, 206-222.
4. P. Sikorski, R. Hori and M. Wada, *Biomacromolecules*, 2009, **10**, 1100-1105.
5. V. L. Deringer, U. Englert and R. Dronskowski, *Biomacromolecules*, 2016, **17**, 996-1003.
6. Y. Nishiyama, P. Langan and H. Chanzy, *Journal of the American Chemical Society*, 2002, **124**, 9074-9082.
7. B. Hess, C. Kutzner, D. van der Spoel and E. Lindahl, *Journal of Chemical Theory and Computation*, 2008, **4**, 435-447.
8. O. Guvench, S. S. Mallajosyula, E. P. Raman, E. Hatcher, K. Vanommeslaeghe, T. J. Foster, F. W. Jamison and A. D. MacKerell, *Journal of Chemical Theory and Computation*, 2011, **7**, 3162-3180.
9. P. Mark and L. Nilsson, *The Journal of Physical Chemistry A*, 2001, **105**, 9954-9960.
10. K. Vanommeslaeghe and A. D. MacKerell, Jr., *Journal of Chemical Information and Modeling*, 2012, **52**, 3144-3154.
11. J. Lee, X. Cheng, J. M. Swails, M. S. Yeom, P. K. Eastman, J. A. Lemkul, S. Wei, J. Buckner, J. C. Jeong, Y. Qi, S. Jo, V. S. Pande, D. A. Case, C. L. Brooks, A. D. MacKerell, J. B. Klauda and W. Im, *Journal of Chemical Theory and Computation*, 2016, **12**, 405-413.
12. T. Darden, D. York and L. Pedersen, *The Journal of Chemical Physics*, 1993, **98**, 10089-10092.
13. W. Humphrey, A. Dalke and K. Schulten, *Journal of Molecular Graphics*, 1996, **14**, 33-38.
14. W. Jiao, L. Li, A. Yu, D. Zhao, B. Sheng, M. Aikelamu, B. Li and X. Zhang, *Journal of Agricultural and Food Chemistry*, 2019, **67**, 927-934.